Genetic screening and metabolomics identify glial adenosine metabolism as a therapeutic target in Parkinson's disease

Sodders MJ[1], Avila-Pacheco J[2], Okorie E[1], Shen M[1], Kumari N[1], Marathi A[1], Lakhani M[1], Bullock K[2], Pierce K[2], Dennis C[2], Jenafavre S[2], Sarkar S[3], Scherzer CR[4,5], Clish C[2], Olsen AL[1,5]

1. Department of Neurology, University of Pittsburgh, Pittsburgh PA
2. Metabolomics Platform, Broad Institute, Boston MA
3. Department of Environmental Medicine, Department of Neuroscience, University of Rochester, Rochester NY
4. Stephen and Denise Adams Center for Parkinson's Disease Research of Yale School of Medicine, New Haven, CT 06511, USA
5. Aligning Science Across Parkinson's (ASAP) Collaborative Research Network, Chevy Chase, MD 20815

Corresponding Author

Abby L. Olsen
BST-3 7017
3501 Fifth Ave
University of Pittsburgh
Pittsburgh, PA 15213
412-648-4678
abby.olsen@pitt.edu

Abstract

Parkinson's disease (PD) is the second most common neurodegenerative disorder and lacks disease-modifying therapies. We developed a *Drosophila* model for identifying novel glial-based therapeutic targets for PD. In this model, human α-synuclein is expressed in neurons and individual genes are independently knocked down in glia. We performed a forward genetic screen, knocking down the entire *Drosophila* kinome in glia in α-synuclein expressing flies. Among the top hits were five genes (*Ak1*, *Ak6*, *Adk1*, *Adk2*, and *awd*) involved in adenosine

metabolism. Knockdown of each gene improved locomotor dysfunction, rescued neurodegeneration, and increased brain adenosine levels. We determined that the mechanism of neuroprotection involves adenosine itself, as opposed to a downstream metabolite. We dove deeper into the mechanism for one gene, *Ak1*, finding rescue of dopaminergic neuron loss, α-synuclein aggregation, and bioenergetic dysfunction after glial *Ak1* knockdown. We performed metabolomics in *Drosophila* and in human PD patients, allowing us to comprehensively characterize changes in purine metabolism and identify potential biomarkers of dysfunctional adenosine metabolism in people. These experiments support glial adenosine as a novel therapeutic target in PD.

Introduction

There are no disease-modifying therapies for Parkinson's disease (PD). Although many known PD risk genes are expressed in glia, the role of individual glial genes in PD pathogenesis is poorly understood. To identify novel glial-based therapeutic targets for PD, we developed a *Drosophila* PD model[1] in which gene expression can be independently manipulated in neurons and glia[2,3] using the Q[4] and UAS-Gal4[5] expression systems (Figure 1A). In this model, wild type human α-synuclein is expressed in all neurons using the pan-neuronal driver *neuronal-synaptobrevin* (*nSyb-QF2*). These flies develop the key hallmarks of PD, including death of dopaminergic neurons, motor impairment, and α-synuclein inclusions. In the glia, any gene of interest can be over-expressed or knocked down using the pan-glial driver *repo-Gal4*. To identify glial genes that either enhance or suppress neuronal α-synuclein toxicity, we performed a forward genetic screen, knocking down the entire *Drosophila* kinome (360 kinases) in glia in α-synuclein flies or control flies. Among the top hits identified in the kinome screen were five genes (*Ak1*, *Ak6*, *Adk1*, *Adk2*, and *awd*) involved in adenosine metabolism, a component of purine metabolism. Expression of purine metabolism genes is dysregulated in PD patient brains[6] and in our *Drosophila* PD model[3,7].

Glial knockdown of *Ak1*, *Ak6*, *Adk1*, *Adk2*, or *awd* resulted in increased adenosine and rescued neurodegeneration in *Drosophila*, suggesting that adenosine may be neuroprotective. Adenosine has many functions, at least two of which are germane to PD: 1) Secreted adenosine can signal through receptors, which have multiple, simultaneous, opposing effects in PD.

Adenosine signaling through the *inhibitory* A_1 receptor *reduces* cAMP production and protects neurons from acute injury[8]. In contrast, adenosine signaling through the *excitatory* A_{2A} receptor *increases* cAMP production. The specific A_{2A} receptor antagonist istradefyelline is an FDA-approved symptomatic therapy for PD, supporting the relevance of this pathway in humans. 2) Adenosine can be metabolized to urate. Low urate is a PD biomarker[9–15], and urate is neuroprotective in models of PD[16–20], but a recent randomized clinical trial designed to increase urate levels failed to slow progression in PD[21]. Thus, while adenosine signaling and metabolism to urate are highly relevant to PD pathology, therapeutic targeting of this complex pathway has not been optimized.

To investigate the mechanism of rescue, we measured adenosine and its downstream metabolites after glial *Ak1*, *Ak6*, *Adk1*, *Adk2*, or *awd* knockdown. These experiments suggested that it is likely adenosine itself, as opposed to a downstream metabolite, that is responsible for rescue of neurodegeneration. We further determined that glial *Ak1* knockdown rescues dopaminergic neuron loss, α-synuclein aggregation, and bioenergetic dysfunction. Finally, we performed metabolomics in both *Drosophila* and in human patients with PD or healthy controls, allowing us to comprehensively characterize changes in purine metabolism and identify potential biomarkers of dysfunctional adenosine metabolism in people with PD.

In summary, through genetic screening and metabolomics in a *Drosophila* model of PD, we have identified adenosine metabolism as a novel potential glial-based therapeutic target for PD. Further, we have identified potential biomarkers of adenosine metabolism dysfunction in patients with PD.

Results

We performed a forward genetic screen, knocking down the entire *Drosophila* kinome (360 kinases) in glia. The primary readout for the screen was a published behavioral assay that is based on locomotion[2]. Without any RNAi present, the average percentage locomotion in this assay for control flies was 67%, and the average percentage locomotion for α-synuclein flies was 44%. Based on results of the locomotion assay, genes were categorized as developmentally lethal, toxic, enhancer, suppressor, or having no effect (Figure 1B). Genes were categorized as developmentally lethal if no flies of the intended genotype eclosed. Suppressors were defined as

those genes whose knockdown resulted in a 25% increase in locomotion in α-synuclein flies (Figure 1B-1D). Enhancers were defined as those genes whose knockdown results in a 25% decrease in locomotion in α-synuclein flies (Figure 1B-1C, Supplemental Figure 1). Toxic genes were defined as those whose knockdown results in a 25% decrease in locomotion in control flies. Any gene not meeting the 25% threshold was categorized as having no effect. A heatmap of the results for all non-lethal genes is shown in Figure 1C and all results are included as Supplemental File 1.

We performed STRING analysis (https://string-db.org, version 12.0) and found two networks among the suppressor genes (Figure 1E). No gene ontology or KEGG pathway analysis terms were statistically significantly enriched when comparing the list of 28 suppressors to the full list of kinases as a reference gene set, but, descriptively, one network consists primarily of purine metabolism related genes and the other of genes related to cell cycle and cell number (Figure 1E). STRING analysis of the enhancers showed one large network and one smaller network (Supplemental Figure 2). As with the suppressors, no gene ontology or KEGG pathway analysis terms were statistically significantly enriched when comparing to the full list of kinases as a reference gene set. Descriptively, most genes in the enhancer networks were involved in cell signaling, and specifically Wnt signaling (Supplemental Figure 2).

We are most interested in the suppressors identified in the kinome screen, as these genes might be able to rescue neurodegeneration if inhibited pharmacologically. Thus, we decided to focus further on the purine metabolism pathway, which has known relevance to Parkinson's disease. Interestingly, among the 10 suppressor genes involved in purine metabolism identified in the kinome screen, 6 are involved specifically in adenosine metabolism, and their knockdown would be predicted to result in increased adenosine levels based on their predicted enzymatic function (Figure 2A). The genes include two adenosine kinases (*Adk1, Adk2*), two adenylate kinases (*Ak1, Ak6*), and two nucleoside diphosphate-kinases (*awd, nmdyn-D6*). Each has a human ortholog with high degree of homology (Figure 2B).

To determine whether knockdown of these 6 genes does increase adenosine, we used a fluorometric assay to measure adenosine levels in *Drosophila* heads (Figure 2C). We found statistically significantly increased adenosine after knockdown of *Ak1*, *Ak6, Adk1*, and *awd*. Knockdown of *Adk2* also led to increased adenosine, though the result was shy of statistical significance ($p = 0.16$). Knockdown of *nmdyn-D6* did not lead to increased adenosine. We

therefore decided to focus the remainder of our analysis on the 5 genes (*Adk1, Adk2, Ak1, Ak2,* and *awd*) whose knockdown both increased adenosine and rescued locomotion in α-synuclein flies. We confirmed that knockdown of each gene rescued locomotion with a second independent RNAi line for 3 of the 5 genes in question, *Ak1, Ak2,* and *awd* (Supplemental Figure 3A). For *Adk1* knockdown, a second line caused toxicity in both control and α-synuclein flies (Supplemental Figure 3A), and for *Adk2*, a second line did not rescue locomotion (Supplemental Figure 3A), presumably due lack of efficient knockdown (Supplemental Figure 3B). Finally, we confirmed that knockdown of each gene rescues neurodegeneration by measuring total cell counts in the anterior medulla, an area of strong pathology in this model (Figure 2D). The collective results provide strong support for adenosine as a novel therapeutic target pathway.

Adenosine has many potential effects, including that it can enter the purine breakdown pathway. In humans and other closely related hominids[22], this pathway ends in metabolism to urate, whereas in nearly all other species, including *Drosophila*, urate is further metabolized to allantoin, and eventually to urea (Figure 3A). Many epidemiologic studies have found low serum or CSF urate levels in PD patients[9–15], and urate has been shown to be neuroprotective in animal models of PD[16–20]. Thus, it is possible that the neuroprotective effects of adenosine are mediated not by adenosine itself, but rather by its metabolism to urate. To better understand the downstream metabolite changes that occur after increasing adenosine, we measured inosine, hypoxanthine/xanthine, and urate levels after knocking down each of the 5 genes (Figure 3B). These experiments identified more modest changes in downstream metabolites after glial knockdown of the 5 genes, all of which were smaller in amplitude than the changes in adenosine, as shown in the heatmap in Figure 3B.

To further explore this, we identified all *Drosophila* genes involved in purine breakdown using the KEGG database (https://www.kegg.jp, release 109.1). We assessed locomotion in control and α-synuclein flies after individually knocking down all but 1 *Drosophila* gene involved in purine breakdown in glia (Figure 3A). One xanthine dehydrogenase, *AOX2*, was not able to be tested due to lack of any publicly available RNAi lines. First, we knocked down the 6 adenosine deaminases (*Adgf-A, Adgf-A2, Adgf-B, Adgf-C, Adgf-D, Adgf-E*), which convert adenosine to inosine (Figure 3A). With the notable exception of *Adgf-C* knockdown, which was toxic in both control and α-synuclein flies, knockdown of adenosine deaminases improved locomotion in α-synuclein flies (Figure 3C). In contrast, knockdown of genes further

downstream in purine breakdown failed to improve locomotion in α-synuclein flies (Figure 3D). Thus, while we cannot exclude neuroprotective roles for inosine, hypoxanthine, xanthine, or urate, our data suggest that the effects are upstream of these metabolites.

To further explore the downstream mechanisms of neuroprotection, we decided to focus on a single gene, adenylate kinase 1 (*Ak1*). We chose *Ak1* over the other genes because of attractive properties that make it an interesting potential therapeutic target. That is, loss of *Ak1* appears to be relatively well-tolerated, as *Ak1*$^{-/-}$ mice are viable and fertile, with only mild stress-induced phenotypes[23–28]. We have already shown that glial *Ak1* knockdown rescues neurodegeneration (Figure 2D). We next confirmed that this includes rescue of dopaminergic neuron loss (Figure 4A). To determine if this mechanism involves α-synuclein, we investigated large α-synuclein aggregates, α-synuclein oligomers, and phosphorylated α-synuclein, finding that *Ak1* knockdown improves each pathologic α-synuclein phenotype (Figure 4B-D). Thus, glial *Ak1* knockdown rescues the two pathologic hallmarks of PD, dopaminergic neuron loss and α-synuclein pathology.

Ak1 is an adenylate kinase, part of a family of enzymes that catalyze the reversible reaction AMP + ATP ↔ 2 ADP. These enzymes are thought to sense the energy state of the cell and help coordinate a response by controlling adenine nucleotide levels[29]. We have previously demonstrated that α-synuclein flies have a quiescent bioenergetic profile, with impairments in both oxidative consumption rate (OCR) and extracellular acidification rate (ECAR), compared to control flies[7]. We show here that glial *Ak1* knockdown rescues the impairment in the OCR (Figure 5A), and partially rescues the impairment in the ECAR (Figure 5B), leading to a more energetic profile similar to the control fly brain.

To characterize changes in purine metabolites following glial *Ak1* knockdown more comprehensively, we performed metabolomics on control or α-synuclein flies, with or without glial *Ak1* knockdown, using a platform that relies on a combination of four liquid chromatography mass spectrometry (LC-MS) methods, which measure both polar and non-polar metabolites. We identified 588 known metabolites. Principal component analysis using known metabolites demonstrated that our samples clustered by genotype (Supplemental Figure 4), with *Ak1* knockdown accounting for 33.59% of the variance and α-synuclein accounting for 15.82% of the variance. For the full *Drosophila* metabolomics data set, see Supplemental File 2.

We next compared known metabolites between control and α-synuclein flies (Figure 6A). We found significant changes in levels of many metabolites, including multiple purine metabolites. Significantly, urate was among the most significantly decreased in α-synuclein flies compared to control flies (Figure 6A). Surprisingly, adenosine was elevated in α-synuclein compared to control flies in this analysis, with a nominally significant p-value of 0.04 (Figure 6A). We performed metabolite set enrichment analysis using Metaboanalyst, finding that purine metabolism was among the statistically significantly enriched pathways that were different between control and α-synuclein flies, along with pterins and derivatives, medium-chain hydroxy acids and derivatives, and amino acids, peptides and analogues (Figure 6B).

We next compared metabolites between α-synuclein + glial *Ak1* knockdown flies and α-synuclein flies with intact Ak1 (Figure 6C). Interestingly, among the most significantly changed metabolites were allantoin, the end-product of purine metabolism in *Drosophila* (Figure 3A), which was increased with glial *Ak1* knockdown in α-synuclein flies. Metabolite set analysis revealed significant enrichment in quinoline carboxylic acids, purines and purine derivatives, and pyrimidines and pyrimidine derivatives (Figure 6D). Thus, the metabolomics data independently identified purine metabolism as a major pathway that is dysregulated between control and α-synuclein flies and rescued by glial *Ak1* knockdown.

To better understand how individual purine metabolites differ among our genotypes, we further examined all purine metabolites identified in the metabolomics study. For this analysis, metabolite levels were normalized on a log10 scale (Supplemental Figure 5A). In total, 29 known purine metabolites were detected in our study. Most of these metabolites were positively correlated among samples (Supplemental Figure 5B). We performed hierarchical clustering among our samples and metabolites, finding that samples correlated more strongly by glial *Ak1* knockdown status than by α-synuclein status (Figure 7A).

To identify significantly changed purine metabolites across the 4 genotypes, we performed one-way ANOVA with corrections for multiple testing (Supplemental File 4). 15 out of the 29 purine metabolites were significantly different (Figure 7A, indicated by # symbol). These fell into 5 groups based on patterns of change. The largest group were metabolites (including adenosine) that were equivalent or slightly higher in α-synuclein than control flies and that were substantially increased following glial *Ak1* knockdown in both α-synuclein and control

flies (Figure 7B). The second group includes metabolites that were higher in α-synuclein flies than in control flies and substantially increased in α-synuclein flies with glial *Ak1* knockdown (Figure 7C). The third group (including xanthine) were metabolites that were lower in α-synuclein than control flies but substantially increased following glial *Ak1* knockdown in both α-synuclein and control flies (Figure 7D). The fourth group (including urate) were metabolites that were substantially lower in α-synuclein than control flies and increased in α-synuclein flies following Ak1 knockdown but *decreased* in control flies following Ak1 knockdown (Figure 7E). The final group were metabolites that were substantially higher in α-synuclein flies than control flies and that were decreased by glial *Ak1* knockdown (Figure 7F). This group includes 1,7-dimethyluric acid, 3-methylxanthine, and 1,3-dimethyluric acid.

Finally, to demonstrate the relevance of the adenosine metabolism pathway to human PD, we performed metabolomics on human cerebrospinal fluid (CSF) samples from patients with PD or healthy controls who were enrolled in the Harvard Biomarkers Study (Figure 8A). Out of 68 metabolites identified, 12 metabolites had a nominally statistically significant p-value, including uric acid ($p < 0.041$) and xanthine ($p < 0.0014$). These data corroborate reports in the literature documenting that PD patients have decreased CSF uric acid compared to controls[30,31], and intriguingly, also identify even stronger changes in xanthine.

In summary, through a combination of genetic screening and metabolomics, we identified glial adenosine metabolism as novel therapeutic target pathway in PD. Further, we identify glial *Ak1* as an especially promising target gene for increasing glial adenosine levels and rescuing neuronal α-synuclein toxicity.

Discussion

We identified 5 genes (*Adk1, Adk2, Ak1, Ak6,* and *awd*) whose knockdown results in increased adenosine and rescues neurodegeneration, suggesting that increasing adenosine is neuroprotective. Of these 5 genes, we chose to focus most on *Ak1* both because of relevance to PD and because of properties that make it a potentially attractive therapeutic target. Both *Ak1* and *Ak6* are adenylate kinases. Their human orthologs are the identically named adenylate kinase 1 (*AK1)* and adenylate kinase 6 (*AK6)*, respectively. Relatively little is known about *AK6*, whereas increased *AK1* expression been associated with Alzheimer's disease (AD) and PD in a handful of studies. Park et. al identified increased Ak1 expression in a mouse model of

Alzheimer's disease in whole brain lysates and further found that AK1 was increased in hippocampal neurons in human post-mortem AD[32]. AK1 expression was not examined specifically in glia, however.[32] Garcia-Esparcia et al reported that *AK1* mRNA was upregulated in frontal cortex in PD patients compared to controls[6]. In this study, the AK1 protein was detected in both neurons and astrocytes, but the cell type responsible for the increased mRNA expression was not investigated[6]. Finally, a recent proteomics study found that AK1 was increased in cerebrospinal fluid (CSF) in patients with PD compared to controls[33]. Despite its high degree of conservation and ubiquitous expression, systemic loss of Ak1 appears to be well-tolerated. *Ak1*$^{-/-}$ mice are viable and fertile, with only mild exercise- or ischemia-induced phenotypes[23–28]. Glial *Ak1* knockdown may represent a "backdoor" to the adenosine metabolism pathway, that is, a way of altering adenosine levels indirectly, without attacking some of the most important enzymes involved in adenosine metabolism, thus avoiding some of the most critical side effects.

The next two genes we identified are *Adk1* and *Adk2*, which are adenosine kinases. They share a single human ortholog, adenosine kinase (*ADK*). ADK reduces adenosine levels by phosphorylating adenosine to AMP, and astrocytic ADK is the most important regulator of ambient adenosine levels[34]. Unfortunately, ADK is a poor therapeutic target: Genetic disruption of *Adk* in mice is lethal due to development of neonatal hepatic steatosis[35], missense mutations in humans cause hypermethioninemia, encephalopathy, and abnormal liver function[36], and initial attempts to inhibit ADK have led to on-target toxicity in the form of cerebral micro-hemorrhages[37]. Thus, preventing adenosine breakdown, at least by means of inhibiting ADK, is not likely to be a viable therapeutic strategy for increasing adenosine levels.

The final gene of interest, *awd*, is a nucleoside diphosphate kinase with many functions. Nucleoside diphosphate kinases transfer phosphates between nucleoside diphosphates and triphosphates. *awd* has high homology with both the human *NME1* gene and the *NME2* gene, and highest homology with a readthrough product named *NME1-NME2*. *NME1*$^{-/-}$ and *NME2*$^{-/-}$ mice are viable, though *NME1*$^{-/-}$ mice have growth retardation, and *NME1/NME2* double knockout mice die at birth from severe anemia[38]. NME1 and NME2 are suppressors of tumor metastasis[39]. *awd* also suppresses metastasis in *Drosophila*[40]. Garcia-Esparcia et al found reduced expression of NME1 in Parkinson's disease substantia nigra[6]. Anatha et. al found that NME1 promoted neurite growth in SH-SY5Y cells and dopaminergic neurons[41], and *awd* is

involved in synaptic vesicle recycling in *Drosophila*[42]. Collectively, these limited studies might argue in favor of increasing NME1 expression rather than reducing it and suggest further that *awd*/*NME1* could have different effects in neurons and glia.

One intriguing hypothesis to emerge from our results is that it may be adenosine itself rather than a downstream metabolite that is neuroprotective, as inhibiting downstream purine breakdown enzymes failed to rescue α-synuclein-induced impaired locomotion. Further exploring this topic is of critical importance in terms of clinical trial design, as attempts are underway to increase urate levels by giving patients dietary inosine in both PD and amyotrophic lateral sclerosis (ALS)[43]. Unfortunately, the phase 3 SURE-PD3 trial closed early due to an interim futility analysis, as clinical progression rates were not significantly different between participants who received inosine versus placebo[21]. Participants who received inosine in the trial had sustained increases in serum urate levels, and a previous phase 2 trial confirmed that dietary inosine also increases CSF urate levels[44], suggesting target engagement, although the differences were greater in women than men on subgroup analysis[31]. While there are many potential reasons for clinical trial failure, because adenosine is upstream of inosine, the inosine supplementation approach will not be successful if low urate levels in PD patients are merely a biomarker of adenosine dysfunction.

Based on our data, adenosine itself is unlikely to be the best biomarker of adenosine metabolism dysfunction, for two reasons. 1) Although glial knockdown of *Ak1*, *Ak6*, *Adk1*, *Adk2*, and *awd* consistently and significantly increased adenosine levels, we found inconsistent baseline differences in adenosine levels between control and α-synuclein flies. We often (but not always) found decreased adenosine in α-synuclein flies compared to control flies when measuring it with a fluorometric assay (Figure 3A), yet our in our metabolomics study adenosine was increased in α-synuclein flies (Figure 6A). These differences may be due to the differences in methodology, and it is possible that highly similar metabolites might complicate the results. 2) Adenosine and inosine were detectable only in the pmol range on direct measurement (Figure 2A, 3B), whereas urate was detectable in the nmol range, and hypoxanthine/xanthine in the mmol range. Further, in the human CSF metabolomics study, adenosine and inosine were not detected, whereas xanthine and urate were both detectable and statistically significantly different between PD patients and controls (Figure 8). Finally, xanthine and urate were increased with glial *Ak1*

knockdown (Figure 3D, 3E, 7D, 7E). Thus, xanthine and urate may represent the best biomarkers for assessing adenosine metabolism dysfunction in a clinical setting.

To further explore potential biomarkers, we looked at levels of all purine metabolites across the 4 genotypes, finding 5 general patterns (Figure 7). Intriguingly, 3 purine metabolites related to xanthine and urate (1,7-Dimethyluric acid, 1,3-Dimethyluric acid, and 3-Methylxanthine) had a unique disease-associated pattern of expression (Supplemental Figure 6B, Figure 7E). That is, 1) they were low in α-synuclein flies compared to control flies, 2) glial *Ak1* knockdown normalized the levels in α-synuclein flies, and 3) glial *Ak1* knockdown had no effect on their levels in control flies. Little is known about these metabolites. They are metabolites of caffeine[45], which has been associated with decreased risk of PD in numerous epidemiologic studies[46], as well as theophylline[47], but they are also formed endogenously. 1-7-Dimethyluric acid has been shown to ameliorate ischemic brain injury in mice[48], and 3-Methylxanthine is associated with higher cognitive performance in older adults[49]. Understanding more about specific purine metabolites in disease contexts is an area for future study.

In summary, we have identified glial adenosine metabolism as a novel potential therapeutic target pathway in PD, and we have identified potential downstream biomarkers of adenosine metabolism dysfunction. These biomarkers respond to glial *Ak1* knockdown, which represents a particularly attractive gene target for inhibition in terms of being well-tolerated and glial-specific.

Methods

Drosophila

All fly crosses and aging were performed at 25 °C. All experiments were performed at 10 days post-eclosion. All experiments include both male and female flies. All experiments include control (*nSyb-QF2, repo-Gal4/+*) and α-synuclein flies (*nSyb-QF2, repo-Gal4, QUAS-α-synuclein/+*), with or without a *UAS-RNAi*. The *nSyb-QF2 Drosophila* stock was provided by Dr. Christopher Potter. Transgenic RNAi stocks were obtained from the Bloomington *Drosophila* Stock Center or from Vienna *Drosophila* Resource Center. Two independent RNAi lines were used to confirm rescue of locomotor impairment following *Ak1*, *Ak6*, or *awd* knockdown: *UAS-Ak1 RNAi TRiP.HMC03355*, *UAS-Ak1 RNAi TRiP.GL00177*, *UAS-Ak6 RNAi*

TRiP.GL00285, UAS-Ak6 RNAi GD14036, UAS-awd RNAi TRiP.GL00013, UAS-awd RNAi TRiP.HMJ02099. The first line listed in each pair was used for all other experiments involving gene knockdown. For the *Adk1* knockdown, only a single RNAi line (*UAS-Adk1 RNAi TRiP.HMC06361*) was used, because a second RNAi line failed to replicate the locomotion result (*UAS-Adk1 RNAi KK107704*), likely due to an off-target toxic effect, as the line was toxic in both control and α-synuclein flies (Supplemental Figure 3A). For the *Adk2* knockdown, only a single RNAi line (*UAS-Adk2 RNAi TRiP.GL00036*) was used, because the second line (*UAS-Adk2 RNAi TRiP.HMC05509*) did not significantly rescue locomotion (Supplemental Figure 3A), likely due to failure of knockdown (Supplemental Figure 3B). Efficiency of knockdown was validated using the systemic da-Gal4 driver.

Kinome screen

A list of all *Drosophila* kinases was obtained from flybase.org. Every fly kinase tested in the screen has at least one human ortholog. One transgenic UAS-RNAi line for each kinase was purchased from the Bloomington *Drosophila* Stock Center. Control or α-synuclein flies were crossed to each transgenic UAS-RNAi line. If no progeny of the intended genotype eclosed in 3 independent crosses, the UAS-RNAi line in question was considered developmentally lethal (Figure 1B). For all other crosses, locomotion was measured in control or α-synuclein flies harboring the UAS-RNAi, using a previously published assay[2]. Results were compared to those of control or α-synuclein flies without any RNAi. Each line was categorized as having no effect, being a suppressor, being an enhancer, or being toxic, based on the degree of change in locomotion with the UAS-RNAi line compared to the control or α-synuclein flies without the RNAi. Suppressors were defined as RNAi lines that caused ≥25% improvement in locomotion in α-synuclein flies compared to the α-synuclein baseline. Enhancers were defined as RNAi lines that caused ≥25% decrement in locomotion in α-synuclein flies compared to the α-synuclein baseline. Toxic lines were defined as lines that caused ≥25% decrement in both α-synuclein flies and control flies compared to their respective baselines. All other results were classified as having no effect. Raw data for the kinome screen are included in Supplemental File 1.

Adenosine, inosine, hypoxanthine/xanthine, and urate assays

Flies were anesthetized, then snap frozen on dry ice to halt metabolic reactions. After freezing, heads were removed and homogenized in assay buffer (Abcam). Homogenates were deproteinized using the Deproteinizing Sample Preparation Kit - TCA (Abcam ab204708). Fluorometric kits for adenosine (Abcam ab211094), inosine (Abcam ab126286), hypoxanthine/xanthine (Abcam ab155900), and urate (Abcam ab65344) were used per the manufacturer's instructions. The hypoxanthine/xanthine kit does not distinguish between hypoxanthine and xanthine. Each experiment included 6 replicates per genotype, with 1 head per replicate for hypoxanthine/xanthine and 2 heads per replicate for the other assays.

Quantification of total cell counts

For knockdown of *Ak1*, *Adk1*, and *awd,* total cells were counted as previously described[50]. Briefly, flies were fixed in formalin (Fisher Scientific SF9804) and embedded in paraffin (Fisher Scientific 83-30). 2 μm serial frontal sections were prepared through the entire fly brain. Slides were processed through xylene (Fisher Scientific X3P-1GAL), ethanols (Fisher Scientific 62-15), and into water, then stained with hematoxylin (Fisher Scientific 22-050-206). Images of the anterior medulla from hematoxylin-stained formalin-fixed paraffin-embedded tissue were captured at 40X magnification using brightfield microscopy. One image per fly and 6 flies per genotype were used for quantification. The nuclei in each tissue section were counted and normalized to the area of the section. For knockdown of *Ak6* and *Adk2*, cells were counted using a modified whole-mount protocol[51]. Briefly, fly brains were dissected, fixed in 4% paraformaldehyde (Fisher AA47392-9M), permeabilized, stained with DAPI (Thermo Fisher D1306), and whole mounted with Slowfade Diamond mounting media (Fisher Scientific S36967). Images of the anterior medulla were captured by confocal microscopy at 20X magnification. One image per fly and 6 flies per genotype were used for quantification. The nuclei were counted and normalized to the area of the section using Fiji version 2.3.0/1.53q.

Quantification of TH+ neuron counts

Fly brains were dissected, fixed in 4% paraformaldehyde, permeabilized, stained with DAPI, and stained with primary anti-tyrosine hydroxylase antibody overnight (1:200, mouse, Immunostar 22941). The next day brains were stained with appropriate secondary antibody and whole mounted. Images of the anterior medulla were captured by confocal microscopy at 20X

magnification. One image per fly and 6 flies per genotype were used for quantification. Images were processed using Fiji version 2.3.0/1.53q. The number of TH+ neurons was normalized to the area of the section.

Quantification of α-synuclein aggregates

α-synuclein aggregates were quantified as previously described[50]. Briefly, flies were fixed in formalin (Fisher Scientific SF9804) and embedded in paraffin (Fisher Scientific 83-30). 4 μm serial frontal sections were prepared through the entire fly brain. Slides were processed through xylene (Fisher Scientific X3P-1GAL), ethanols (Fisher Scientific 62-15), and into water. Microwave antigen retrieval with 10 mM sodium citrate (Fisher Scientific S279-3), pH 6.0, was performed. Slides were blocked in 2% milk (Millipore Sigma M7409) in PBS (Fisher Scientific BP665-1) with 0.3% triton X-100 (Thermo Scientific AAA16046AP) for 1 hour then incubated with anti-α-synuclein 5G4 antibody (1:50,000, mouse, Millipore MABN389) in 2% milk in PBS with 0.3% triton X-100 at room temperature overnight. Slides were incubated with fluorophore-conjugated secondary antibody in 2% milk in PBS with 0.3% triton X-100 for 1 hour (1:200, Alexa 555, Invitrogen A-21424) then mounted with DAPI-containing Fluoromount medium (Southern Biotech 0100-20). Immunofluorescence microscopy was performed on a Zeiss LSM 800 confocal microscope. Images of the anterior medulla from immunofluorescence-stained formalin-fixed paraffin-embedded tissue were captured on a confocal microscope at 63X magnification. One image per fly and 6 flies per genotype were used for quantification. The α-synuclein aggregates in each tissue section were counted and normalized to the area of the section. Images were processed using Fiji version 2.3.0/1.53q.

Western blotting

Fly heads were dissected then homogenized in 2X Laemmli buffer (Sigma Aldrich S3401), boiled for 10 minutes, and centrifuged. SDS-PAGE was performed (Bio-Rad) followed by transfer to 0.2 μm nitrocellulose membrane (Bio-Rad 1704270) and microwave antigen retrieval in PBS. Membranes were blocked in 2% milk in PBS with 0.05% Tween-20 (Fisher PI85114) for 1 hour, then immunoblotted with appropriate primary antibody in 2% milk in PBS with 0.05% Tween-20 overnight at 4 °C. Primary antibodies used include α-synuclein H3C (1:10,000 to 1:100,000, mouse, Developmental Studies Hybridoma Bank H3C), α-synuclein clone 42

(1:5,000 mouse, BD Bioscience), and phospho-serine 129 α-synuclein (1:5,000, rabbit, Abcam ab51253). Membranes were incubated with appropriate horseradish peroxidase-conjugated secondary antibodies (1:50,000) in 2% milk in PBS with 0.05% Tween-20 for 3 hours. Signal was developed with enhanced chemiluminescence (Thermo Fisher 32106).

Oligomer assay

As previously published[3], 20 fly heads per genotype were homogenized in 20 ul TNE lysis buffer (10 mm Tris HCl, 150 mM NaCl, 5 mM EGTA, 0.5% nonidet-40) supplemented with HALT protease and phosphatase inhibitor (Fisher Scientific 78440). The homogenate was briefly spun down to remove debris. The remaining supernatant was ultracentrifuged at 100,000 x g for 1 hour at 4° C. The supernatant was transferred to a new tube and combined with 2X Laemmli buffer (Sigma Aldrich S3401) at a 1:1 ratio. SDS-PAGE was then performed as above, except without boiling samples and without microwave antigen retrieval.

Locomotion assay

Adult flies were aged in vials containing 9-20 flies per vial. At day 10 post-eclosion, flies were transferred to a clean vial (without food) and given 1 minute to acclimate to the new vial. The vial was then gently tapped three times to trigger the startle-induced locomotion response, then placed on its side for 15 seconds. The percentage of flies still in motion was then recorded. Differences between genotypes were measured and statistical significance assessed by two-way ANOVA using GraphPad Prism version 10.2.3.

Seahorse assay

The OCR and extracellular acidification rate were measured using a Seahorse XFe96 metabolic analyzer. Brains were dissected and plated at one brain per well on Seahorse XFe96 flux pack plates (Agilent 103793-100) following the manufacturer's protocol and as previously published[7]. The OCR values were normalized to DNA content using a CyQUANT assay (ThermoFisher C7026) following the manufacturer's protocol.

Quantitative real-time qPCR

Gene knockdown was confirmed using qRT-PCR. Primers were chosen from the DRSC FlyPrimerBank [52]. 6 heads per genotype were used. Total RNA was prepared with Qiazol (Qiagen 79306) per the manufacturer's instructions then treated with DNase (Thermo Fisher EN0521) for 15 minutes. cDNA was prepared using a High Capacity cDNA Reverse Transcription Kit (Applied Biosystems 43-688-14), then amplified with SYBR green (Bio-Rad 1708882) on a StepOne Plus Real-Time PCR system (Applied Biosystems 4376600). Relative expression was determined using the ΔΔCt method, with normalization to *RPL32* used as a housekeeping gene.

Drosophila Metabolomics

Metabolomics on fly heads was performed using a platform that relies on a combination of four non-targeted liquid chromatography mass spectrometry (LC-MS) methods which measure both polar and non-polar metabolites[53]. n = 3 replicates per genotype of 25 fly heads each. Sample homogenates were generated by homogenizing the fly heads in 100 µL water using a TissueLyser II (QIAGEN) bead mill set to two 2 min intervals at 20. The metabolomics results included 567 known metabolites confirmed by i) matching measured retention times and masses to mixtures of reference metabolites analyzed in each batch; and ii) matching an internal database of >600 compounds that have been characterized using the profiling methods applied on this study. While the non-targeted methods used in this platform generate thousands of signals from unidentified compounds, for purposes of this manuscript, we focused our analysis on the known metabolites. The full metabolomics data set is included in Supplemental Table 2.

Principal component analysis was performed using R version 4.3.1. Volcano plots of significantly changed metabolites between different pairwise combinations were generated in R. Metabolite enrichment analysis and hierarchical clustering of samples was created with Metaboanalyst 6.0 (https://www.metaboanalyst.ca). Changes in individual purine metabolite levels were graphed with Metaboanlyst 6.0.

Human CSF metabolomics

The Harvard Biomarkers Study (HBS) is a case-control study including 3,000 patients with various neurodegenerative diseases as well as healthy controls (HC). Informed consent was

obtained for all participants. The study protocol was approved by the institutional review board of Mass General Brigham. The metabolomics analysis was performed on a subset of patients from the study. Characteristics are shown in Figure 8A. Human CSF was analyzed with BASF Metabolome Solutions GmbH. Data were normalized to the median of pooled samples to account for process variability. 64 metabolites were identified, of which 48 were known and 6 unknown.

Statistics

All statistical analysis aside from the metabolomics was performed using GraphPad Prism version 10.1.

Data availability

The data that support the findings of this study are available from the corresponding author upon request. The supplemental files associated with this manuscript have been deposited in Zenodo: https://doi.org/10.5281/zenodo.11370503

Acknowledgments

The research was funded in part by Aligning Science Across Parkinson's [ASAP-000301] through the Michael J. Fox Foundation for Parkinson's Research (MJFF). For the purpose of open access, the author has applied a CC BY public copyright license to all All Author Accepted Manuscripts arising from this submission.

Other sources of funding include K08NS109344 (Olsen), 5P30AG062421 (Olsen), 2021A003323 the George C. Cotzias Award from the American Parkinson's Disease Association (Olsen), R00ES033723 (Sarkar), P30ES001247 (Sarkar), and AWD00007930 Alzheimer's Association Research Fellowship to Promote Diversity (Kumari).

The HC3 α-synuclein antibody was provided by the Developmental Studies Hybridoma Bank, created by the NICHD of the NIH and maintained at The University of Iowa, Department of Biology, Iowa City, IA 52242. Drosophila stocks obtained from the Bloomington Drosophila Stock Center (NIH P40OD018537) were used in this study. We thank the Transgenic RNAi

Project (TRiP) at the Harvard Medical School (NIH-NIGMS R01GM084947) for making transgenic RNAi stocks.

Figure Legends

Figure 1: A kinome screen identifies purine metabolism as a glial therapeutic target pathway. A. Schematic of *Drosophila* model. Human α-synuclein is expressed in neurons, and genes are knocked down independently in glia. B. Percentage of lines characterized as suppressors, enhancers, toxic, lethal, or having no effect. C. Each line in the heatmap represents an individual kinase. D. Enlarged heatmaps demonstrating the suppressors. Statistical significance was determined by comparing the α-synuclein + RNAi of interest to the α-synuclein with no RNAi condition using two-way ANOVA with correction for multiple comparison testing with a false discovery rate of 0.5. *** = q-value <0.005, ** = q-value < 0.01, * = q-value < 0.05. q-values and original p-values for all lines are shown in Supplemental File 1. E. STRING analysis of the suppressors identifies two gene networks. Selected gene ontology and KEGG terms characterizing these genes are shown.

Figure 2: Glial knockdown of *Adk1, Adk1, Ak1, Ak6,* and *awd* increases adenosine and rescues neurodegeneration. A. Schematic of suppressor genes identified in the kinome screen whose knockdown is predicted to increase adenosine. B. Human orthologs of each gene. C. Adenosine was measured using a fluorometric assay. n = 6 heads per genotype. Statistical differences were determined by one-way ANOVA with Dunnett's corrections for multiple comparison testing. ** = p <0.01, * = p <0.05. D. Cells were counted in the anterior medulla and normalized by area. n = 6 flies per genotype. Statistical significance was determined by comparing the α-synuclein + RNAi of interest to the α-synuclein with no RNAi condition using two-way ANOVA with Dunnett's correction for multiple comparison testing. **** = p < 0.001, *** = p < 0.005, ** = p < 0.01, * = p < 0.05.

Figure 3: Rescue of neurodegeneration is likely mediated by adenosine rather downstream metabolites. A. Schematic of metabolites (ovals) and enzymes (boxes) involved in adenosine breakdown. Urate is the end-product of adenosine metabolism in humans. B. Heat map

demonstrating relative change in adenosine metabolites after gene knockdown. C. Statistical significance was determined by comparing the α-synuclein + RNAi of interest to the α-synuclein with no RNAi condition using two-way ANOVA with correction for multiple comparison testing with a false discovery rate of 0.5. **** = q-value < 0.0001, *** = q-value <0.005, ** = q-value < 0.01, * = q-value < 0.05. D. Heatmap of locomotion after gene knockdown. No genes are statistically significant.

Figure 4: Glial Ak1 knockdown rescues dopaminergic neuron loss and pathologic α-synuclein. A. Dissected *Drosophila* brains were stained with tyrosine hydroxylase antibody (Immunostar, 1:200) and appropriate secondary. TH+ neurons in the anterior medulla were counted on 1 confocal slice at 20x magnification and normalized by area. n = 6 flies per genotype. B. Fixed tissue stained with anti-α-synuclein (clone 5G4, 1:50,000, mouse, Millipore) antibody that preferentially recognizes aggregated α-synuclein. Tissue is also stained with DAPI. Representative images are shown on the left. Scale bar = 10 um. Aggregates were counted and normalized by area (right). n = 6 flies per genotype. Total and serine 129 phosphorylated α-synuclein was assessed by immunoblotting with α-synuclein H3C (1:10,000, mouse, Developmental Studies Hybridoma Bank), and phospho-serine 129 α-synuclein (1:5,000, rabbit, Abcam). Bands were quantified using Fiji (right). D. Representative immunoblot (left) stained with anti-α-synuclein clone 42 (1:5,000 mouse, BD Bioscience). The immunoblot was cut to allow for longer exposure for the oligomers compared to the α-synuclein monomer. Oligomers were quantified from 4 independent experiments using Fiji (right).

Figure 5: Glial Ak1 knockdown rescues bioenergetic dysfunction in α-synuclein flies. A. Oxygen consumption rate (OCR). Statistical differences were determined by two-way ANOVA with Dunnett's corrections for multiple comparison testing. *** = p < 0.005, ** = p < 0.01, * = p < 0.05. B. Extracellular acidification rate (ECAR). Statistical differences were determined by two-way ANOVA with Dunnett's corrections for multiple comparison testing. * = p < 0.05. C. Energetic profile. n = 6 flies per genotype.

Figure 6: Metabolomics identifies differences in purine metabolite profiles. n = 3 replicates per genotype of 20 heads each. A. Volcano plot of known metabolites comparing α-synuclein to

control flies. Labeled metabolites (pink dots) have log2 fold change > 0.5 and -log2 p-value > 4. p-values were calculated by Student's t-test between control and α-synuclein flies. B. Metabolite set enrichment was performed in Metaboanalyst. 4 pathways are statistically different between control and α-synuclein flies. C. Volcano plot of known metabolites comparing α-synuclein to control flies. Labeled metabolites (pink dots) have log2 fold change > 0.5 and -log2 p-value > 4. p-values were calculated by Student's t-test between α-synuclein flies with Ak1 knockdown compared to α-synuclein flies with no RNAi. D. Metabolite set enrichment was performed in Metaboanalyst. Three pathways are statistically different between α-synuclein flies with Ak1 knockdown compared to α-synuclein flies with no RNAi.

Figure 7: There are several possible biomarkers for adenosine metabolism dysfunction. A. Hierarchical clustering of 29 purine metabolites across 4 genotypes was performed in Metaboanalyst reveals 15 significantly different metabolites using one-way ANOVA with Fisher's test for multiple comparison testing. The metabolites have 4 patterns of expression, indicated by green, orange, yellow, and blue annotation. B. Most purines are equivalent or slightly higher in α-synuclein than control flies and are substantially increased following glial *Ak1* knockdown in both α-synuclein and control flies. C. Three purines are higher in α-synuclein than control flies and are disproportionately increased following glial *Ak1* knockdown in α-synuclein flies. D. Two purines are lower in α-synuclein than control flies but substantially increased following glial *Ak1* knockdown in both α-synuclein and control flies. E. Two purines are substantially lower in α-synuclein than control flies and increased in α-synuclein flies following Ak1 knockdown but decreased in control flies following Ak1 knockdown. F. Three purines are substantially higher in α-synuclein flies than in control flies and normalized by glial *Ak1* knockdown.

Figure 8: Human CSF metabolomics suggests xanthine and urate as biomarkers. A. Characteristics of study participants. B. Metabolomics results. Full results are included in Supplemental File 3.

Supplemental Figure 1: Heatmap of enhancers from the kinome screen. Statistical significance was determined by comparing the α-synuclein + RNAi of interest to the α-synuclein with no RNAi condition using two-way ANOVA with correction for multiple comparison testing with a false discovery rate of 0.5. *** = q-value <0.005, ** = q-value < 0.01, * = q-value < 0.05. q-values and original p-values for all lines are shown in Supplemental File 1.

Supplemental Figure 2: STRING network analysis of enhancers from the kinome screen. Selected gene ontology and KEGG terms characterizing these genes are shown.

Supplemental Figure 3: A. Locomotion was measured with an independent RNAi-line. n = 6 vials per genotype of 9-20 flies per vial. Statistical significance was determined by comparing the α-synuclein + RNAi of interest to the α-synuclein with no RNAi condition using two-way ANOVA with Dunnett's correction for multiple comparison testing. **** = $p < 0.001$, *** = $p < 0.005$, ** = $p < 0.01$, * = $p < 0.05$. B. Validation of gene knockdown for all RNAi lines. N = 6 heads per genotype. Expression of each gene in control was normalized to a level of 1, and statistical significance was determined by one sample t-test comparing the expression of each gene after knockdown to a theoretical mean of 1. Efficiency of knockdown was validated by crossing each RNAi line to *da-Gal4* driver.

Supplemental Figure 4: Principal component analysis from *Drosophila* metabolomics. Principal component analysis was performed in R using all known metabolites.

Supplemental Figure 5: Purine metabolites are highly correlated. 29 purine metabolites were identified. A. Peak intensity levels of metabolites were normalized in Metaboanalyst using log transformation. B. Hierarchical clustering of normalized data was performed in Metaboanalyst.

Supplemental File 1: Complete results of kinome screen.
Supplemental File 2: Complete results of *Drosophila* metabolomics.
Supplemental File 3: Complete results of human CSF metabolomics.
Supplemental File 4: One-way ANOVA of purine metabolites.

References

1. Ordonez, D. G., Lee, M. K. & Feany, M. B. α-synuclein Induces Mitochondrial Dysfunction through Spectrin and the Actin Cytoskeleton. *Neuron* **97**, 108-124.e6 (2018).
2. Olsen, A. L. & Feany, M. B. Glial α-synuclein promotes neurodegeneration characterized by a distinct transcriptional program in vivo. *Glia* **67**, 1933–1957 (2019).
3. Olsen, A. L. & Feany, M. B. Parkinson's disease risk genes act in glia to control neuronal α-synuclein toxicity. *Neurobiol Dis* **159**, 105482 (2021).
4. Potter, C. J., Tasic, B., Russler, E. V., Liang, L. & Luo, L. The Q system: a repressible binary system for transgene expression, lineage tracing, and mosaic analysis. *Cell* **141**, 536–548 (2010).
5. Brand, A. H. & Perrimon, N. Targeted gene expression as a means of altering cell fates and generating dominant phenotypes. *Development* **118**, 401–415 (1993).
6. Garcia-Esparcia, P., Hernández-Ortega, K., Ansoleaga, B., Carmona, M. & Ferrer, I. Purine metabolism gene deregulation in Parkinson's disease. *Neuropathol. Appl. Neurobiol.* **41**, 926–940 (2015).
7. Sarkar, S. *et al.* Comparative proteomic analysis highlights metabolic dysfunction in α-synucleinopathy. *NPJ Parkinsons Dis* **6**, 40 (2020).
8. Cunha, R. A. How does adenosine control neuronal dysfunction and neurodegeneration? *J Neurochem* **139**, 1019–1055 (2016).
9. Chang, H., Wang, B., Shi, Y. & Zhu, R. Dose-response meta-analysis on urate, gout, and the risk for Parkinson's disease. *NPJ Parkinsons Dis* **8**, 160 (2022).

10. Yakhine-Diop, S. M. S. *et al.* Metabolic alterations in plasma from patients with familial and idiopathic Parkinson's disease. *Aging (Albany NY)* **12**, 16690–16708 (2020).
11. Johansen, K. K. *et al.* Metabolomic profiling in LRRK2-related Parkinson's disease. *PLoS ONE* **4**, e7551 (2009).
12. Shen, C., Guo, Y., Luo, W., Lin, C. & Ding, M. Serum urate and the risk of Parkinson's disease: results from a meta-analysis. *Can J Neurol Sci* **40**, 73–79 (2013).
13. Davis, J. W. *et al.* Observations on serum uric acid levels and the risk of idiopathic Parkinson's disease. *Am J Epidemiol* **144**, 480–484 (1996).
14. de Lau, L. M. L., Koudstaal, P. J., Hofman, A. & Breteler, M. M. B. Serum uric acid levels and the risk of Parkinson disease. *Ann Neurol* **58**, 797–800 (2005).
15. Wen, M. *et al.* Serum uric acid levels in patients with Parkinson's disease: A meta-analysis. *PLoS One* **12**, e0173731 (2017).
16. Bao, L.-H. *et al.* Urate inhibits microglia activation to protect neurons in an LPS-induced model of Parkinson's disease. *J Neuroinflammation* **15**, 131 (2018).
17. Bi, M., Jiao, Q., Du, X. & Jiang, H. Glut9-mediated Urate Uptake Is Responsible for Its Protective Effects on Dopaminergic Neurons in Parkinson's Disease Models. *Front Mol Neurosci* **11**, 21 (2018).
18. Kim, H. N., Shin, J. Y., Kim, D. Y., Lee, J. E. & Lee, P. H. Priming mesenchymal stem cells with uric acid enhances neuroprotective properties in parkinsonian models. *J Tissue Eng* **12**, 20417314211004816 (2021).
19. Lee, J. E. *et al.* Uric Acid Enhances Neurogenesis in a Parkinsonian Model by Remodeling Mitochondria. *Front Aging Neurosci* **14**, 851711 (2022).

20. Nakashima, A. *et al.* Feeding-produced subchronic high plasma levels of uric acid improve behavioral dysfunction in 6-hydroxydopamine-induced mouse model of Parkinson's disease. *Behav Pharmacol* **30**, 89–94 (2019).
21. Parkinson Study Group SURE-PD3 Investigators *et al.* Effect of Urate-Elevating Inosine on Early Parkinson Disease Progression: The SURE-PD3 Randomized Clinical Trial. *JAMA* **326**, 926–939 (2021).
22. Kratzer, J. T. *et al.* Evolutionary history and metabolic insights of ancient mammalian uricases. *Proc Natl Acad Sci U S A* **111**, 3763–3768 (2014).
23. Janssen, E. *et al.* Adenylate kinase 1 deficiency induces molecular and structural adaptations to support muscle energy metabolism. *J. Biol. Chem.* **278**, 12937–12945 (2003).
24. Janssen, E. *et al.* Adenylate kinase 1 gene deletion disrupts muscle energetic economy despite metabolic rearrangement. *EMBO J* **19**, 6371–6381 (2000).
25. Guigas, B. No lack of contraction-induced AMPK activation and glucose uptake in fast-twitch muscles from adenylate kinase-1 knockout mice. *Acta Physiol (Oxf)* **192**, 337 (2008).
26. Zhang, S.-J. *et al.* Activation of glucose transport and AMP-activated protein kinase during muscle contraction in adenylate kinase-1 knockout mice. *Acta Physiol (Oxf)* **192**, 413–420 (2008).
27. Makarchikov, A. F. *et al.* Adenylate kinase 1 knockout mice have normal thiamine triphosphate levels. *Biochim. Biophys. Acta* **1592**, 117–121 (2002).
28. Dzeja, P. P., Bast, P., Pucar, D., Wieringa, B. & Terzic, A. Defective metabolic signaling in adenylate kinase AK1 gene knock-out hearts compromises post-ischemic coronary reflow. *J. Biol. Chem.* **282**, 31366–31372 (2007).

29. Dzeja, P. & Terzic, A. Adenylate kinase and AMP signaling networks: metabolic monitoring, signal communication and body energy sensing. *Int J Mol Sci* **10**, 1729–1772 (2009).

30. Crotty, G. F., Ascherio, A. & Schwarzschild, M. A. Targeting urate to reduce oxidative stress in Parkinson disease. *Exp Neurol* **298**, 210–224 (2017).

31. Schwarzschild, M. A. *et al.* Sex differences by design and outcome in the Safety of Urate Elevation in PD (SURE-PD) trial. *Neurology* **93**, e1328–e1338 (2019).

32. Park, H. *et al.* Neuropathogenic role of adenylate kinase-1 in Aβ-mediated tau phosphorylation via AMPK and GSK3β. *Hum Mol Genet* **21**, 2725–2737 (2012).

33. Kaiser, S. *et al.* A proteogenomic view of Parkinson's disease causality and heterogeneity. *NPJ Parkinsons Dis* **9**, 24 (2023).

34. Arch, J. R. & Newsholme, E. A. Activities and some properties of 5'-nucleotidase, adenosine kinase and adenosine deaminase in tissues from vertebrates and invertebrates in relation to the control of the concentration and the physiological role of adenosine. *Biochem J* **174**, 965–977 (1978).

35. Boison, D. *et al.* Neonatal hepatic steatosis by disruption of the adenosine kinase gene. *Proc Natl Acad Sci U S A* **99**, 6985–6990 (2002).

36. Bjursell, M. K. *et al.* Adenosine kinase deficiency disrupts the methionine cycle and causes hypermethioninemia, encephalopathy, and abnormal liver function. *Am J Hum Genet* **89**, 507–515 (2011).

37. Jarvis, M. F. Therapeutic potential of adenosine kinase inhibition-Revisited. *Pharmacol Res Perspect* **7**, e00506 (2019).

38. Boissan, M. & Lacombe, M.-L. Learning about the functions of NME/NM23: lessons from knockout mice to silencing strategies. *Naunyn Schmiedebergs Arch Pharmacol* **384**, 421–431 (2011).

39. Pamidimukkala, N. *et al.* Nme1 and Nme2 genes exert metastasis-suppressor activities in a genetically engineered mouse model of UV-induced melanoma. *Br J Cancer* **124**, 161–165 (2021).

40. Nallamothu, G., Woolworth, J. A., Dammai, V. & Hsu, T. Awd, the homolog of metastasis suppressor gene Nm23, regulates Drosophila epithelial cell invasion. *Mol Cell Biol* **28**, 1964–1973 (2008).

41. Anantha, J. *et al.* NME1 Protects Against Neurotoxin-, α-Synuclein- and LRRK2-Induced Neurite Degeneration in Cell Models of Parkinson's Disease. *Mol Neurobiol* **59**, 61–76 (2022).

42. Krishnan, K. S. *et al.* Nucleoside diphosphate kinase, a source of GTP, is required for dynamin-dependent synaptic vesicle recycling. *Neuron* **30**, 197–210 (2001).

43. Walk, D. *et al.* Randomized trial of inosine for urate elevation in amyotrophic lateral sclerosis. *Muscle Nerve* **67**, 378–386 (2023).

44. Parkinson Study Group SURE-PD Investigators *et al.* Inosine to increase serum and cerebrospinal fluid urate in Parkinson disease: a randomized clinical trial. *JAMA Neurol* **71**, 141–150 (2014).

45. Rybak, M. E., Sternberg, M. R., Pao, C.-I., Ahluwalia, N. & Pfeiffer, C. M. Urine excretion of caffeine and select caffeine metabolites is common in the U.S. population and associated with caffeine intake. *J Nutr* **145**, 766–774 (2015).

46. Bakshi, R. *et al.* Associations of Lower Caffeine Intake and Plasma Urate Levels with Idiopathic Parkinson's Disease in the Harvard Biomarkers Study. *J Parkinsons Dis* **10**, 505–510 (2020).

47. Kuroda, Y. *et al.* Age-Associated Theophylline Metabolic Activity Corresponds to the Ratio of 1,3-Dimethyluric Acid to Theophylline in Mice. *Biol Pharm Bull* **42**, 1423–1427 (2019).

48. Haberman, F. *et al.* Soluble neuroprotective antioxidant uric acid analogs ameliorate ischemic brain injury in mice. *Neuromolecular Med* **9**, 315–323 (2007).

49. Liu, C. Targeting the cholinergic system in Parkinson's disease. *Acta Pharmacol Sin* **41**, 453–463 (2020).

50. Olsen, A. L., Clemens, S. G. & Feany, M. B. Nicotine-Mediated Rescue of α-Synuclein Toxicity Requires Synaptic Vesicle Glycoprotein 2 in Drosophila. *Mov Disord* (2022) doi:10.1002/mds.29283.

51. Behnke, J. A., Ye, C., Moberg, K. H. & Zheng, J. Q. A protocol to detect neurodegeneration in Drosophila melanogaster whole-brain mounts using advanced microscopy. *STAR Protoc* **2**, 100689 (2021).

52. Hu, Y. *et al.* FlyPrimerBank: an online database for Drosophila melanogaster gene expression analysis and knockdown evaluation of RNAi reagents. *G3 (Bethesda)* **3**, 1607–1616 (2013).

53. Li, C. *et al.* Gut microbiome and metabolome profiling in Framingham heart study reveals cholesterol-metabolizing bacteria. *Cell* **187**, 1834-1852.e19 (2024).

Figure 1

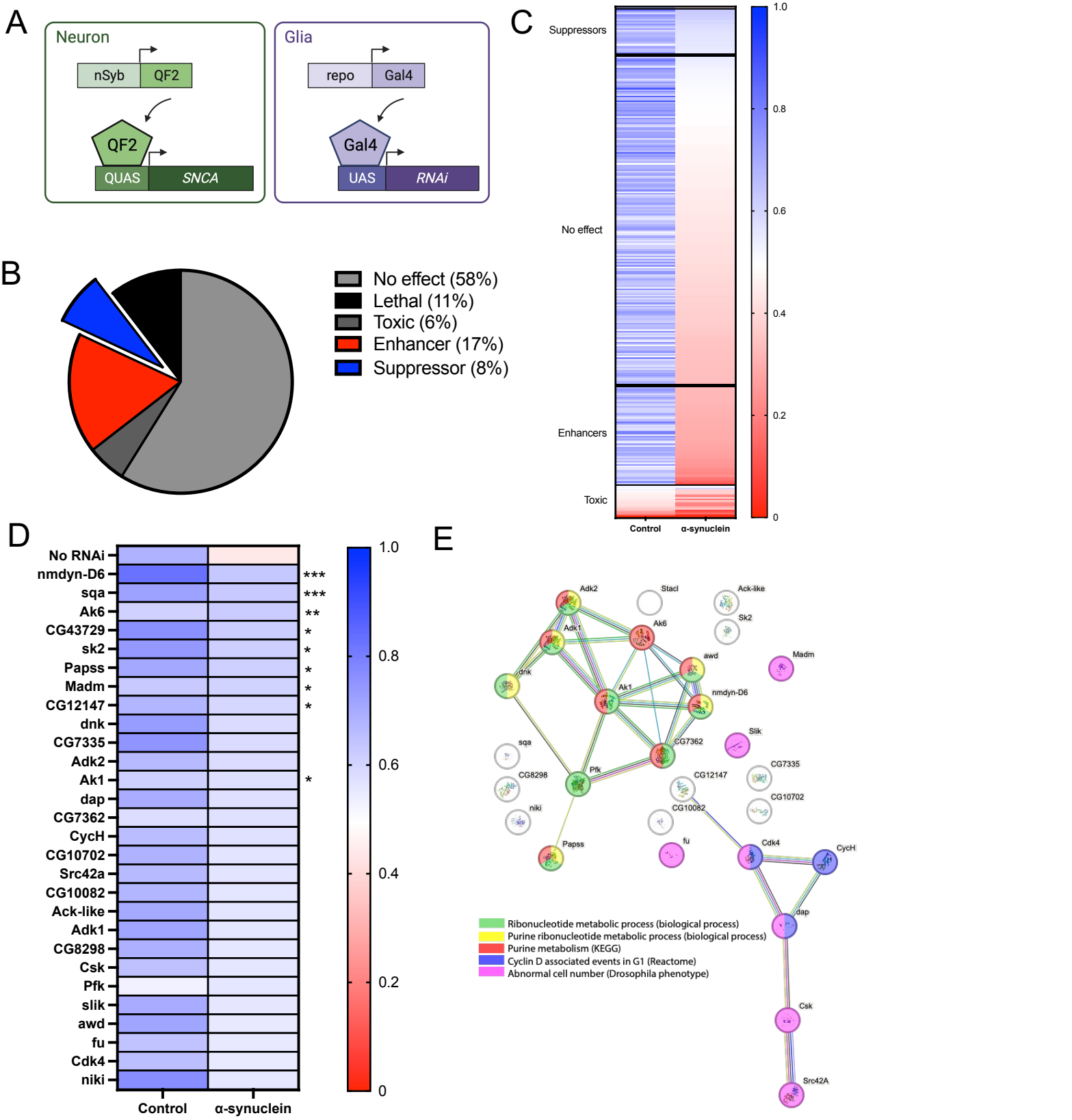

Figure 2

A

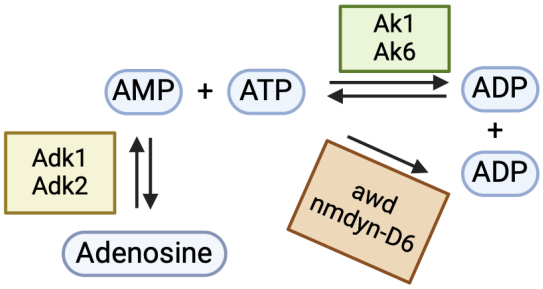

B

Drosophila Gene	Best human ortholog
Adk1	ADK
Adk2	ADK
Ak1	AK1
Ak6	AK6
awd	NME1—NME2
nmdyn-D6	NME6

C

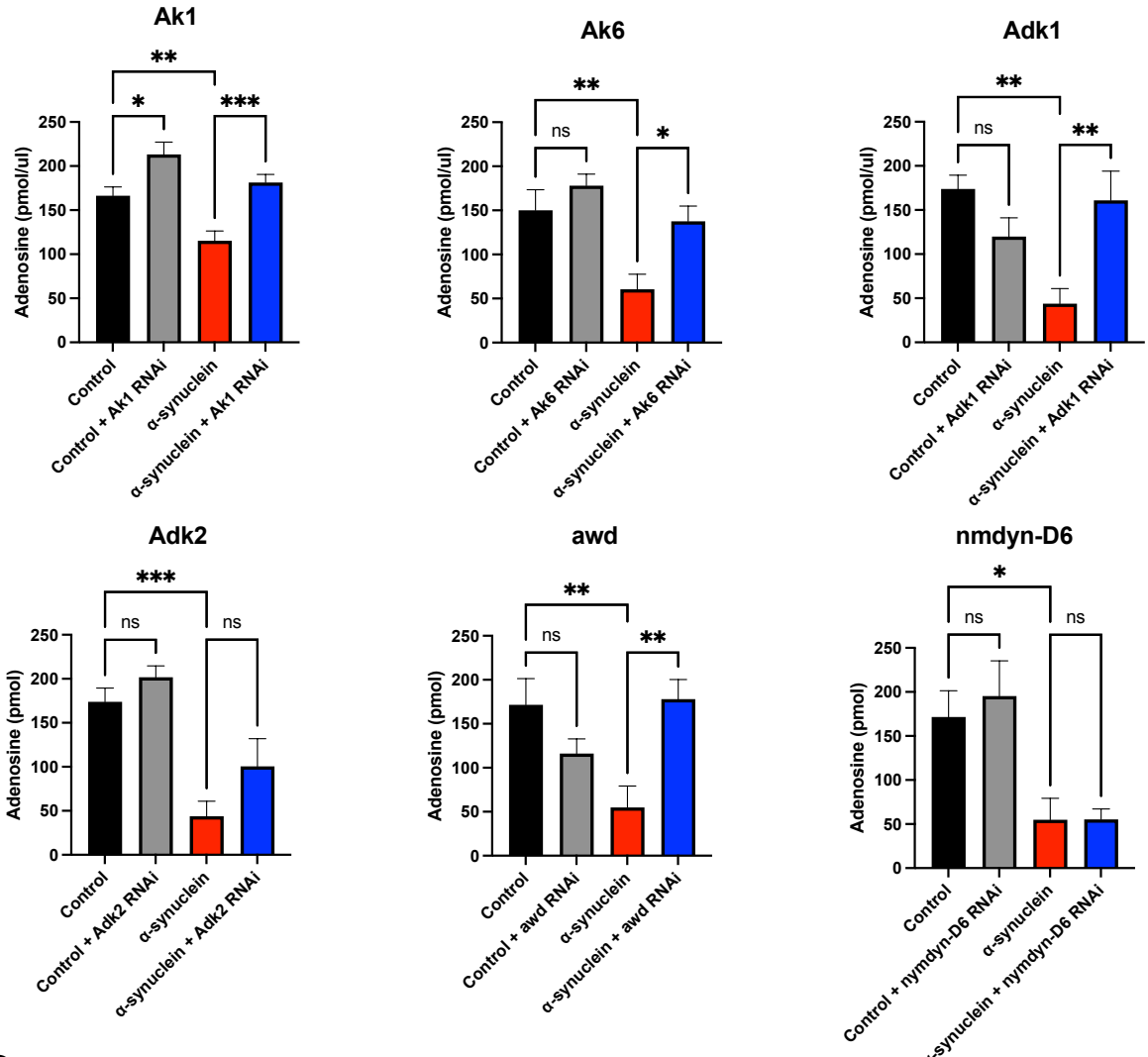

D

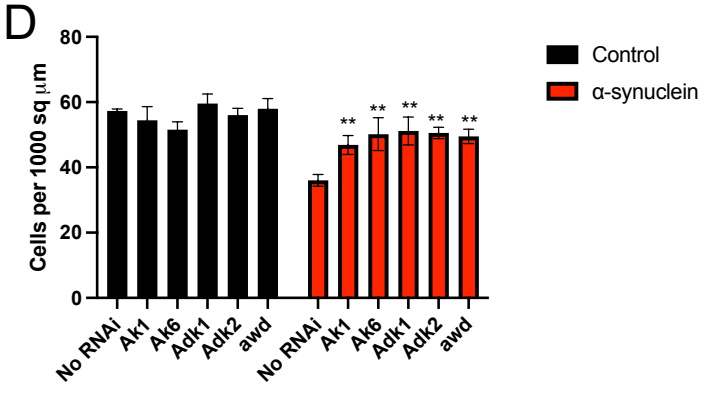

Figure 3

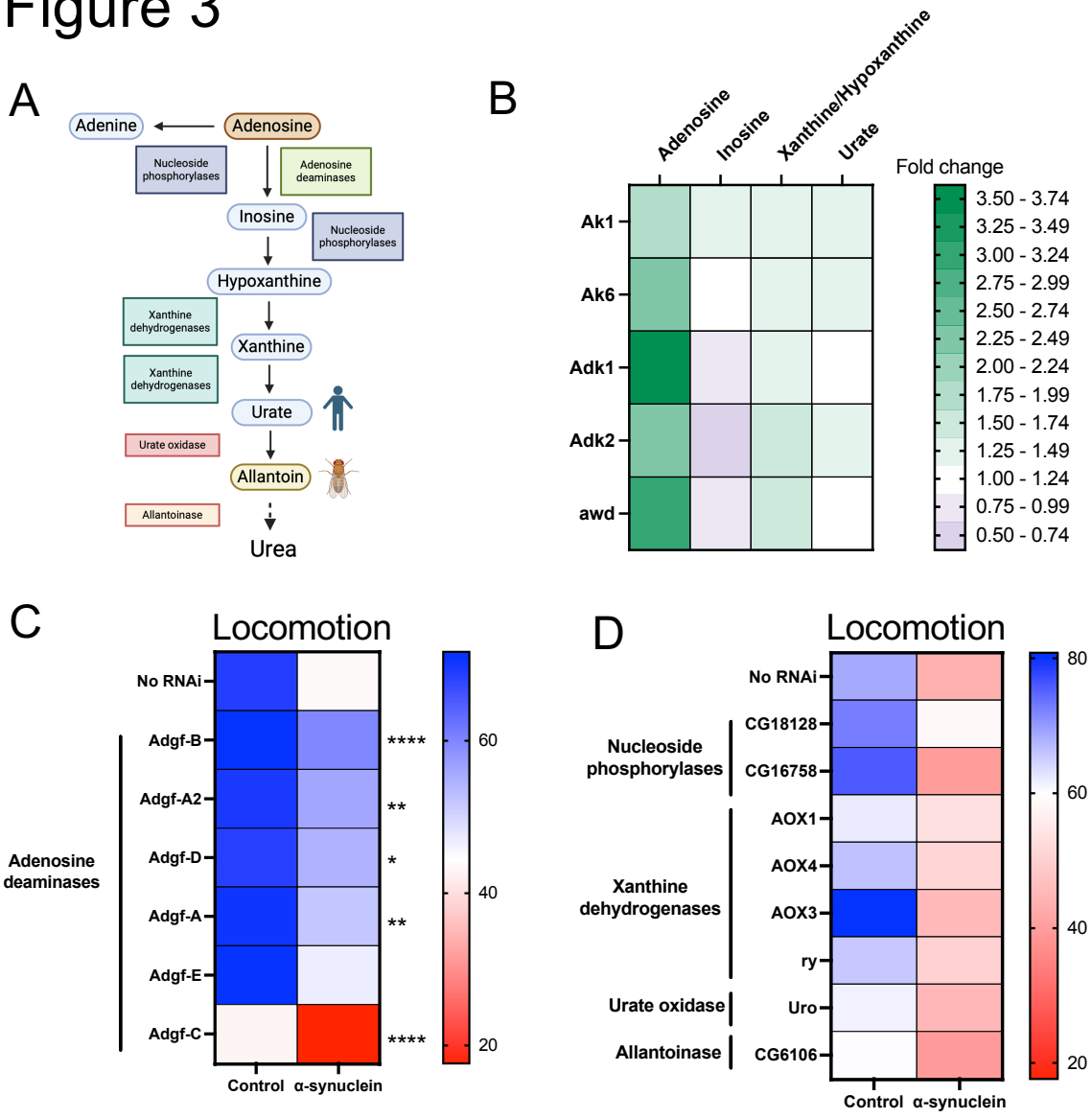

Figure 4

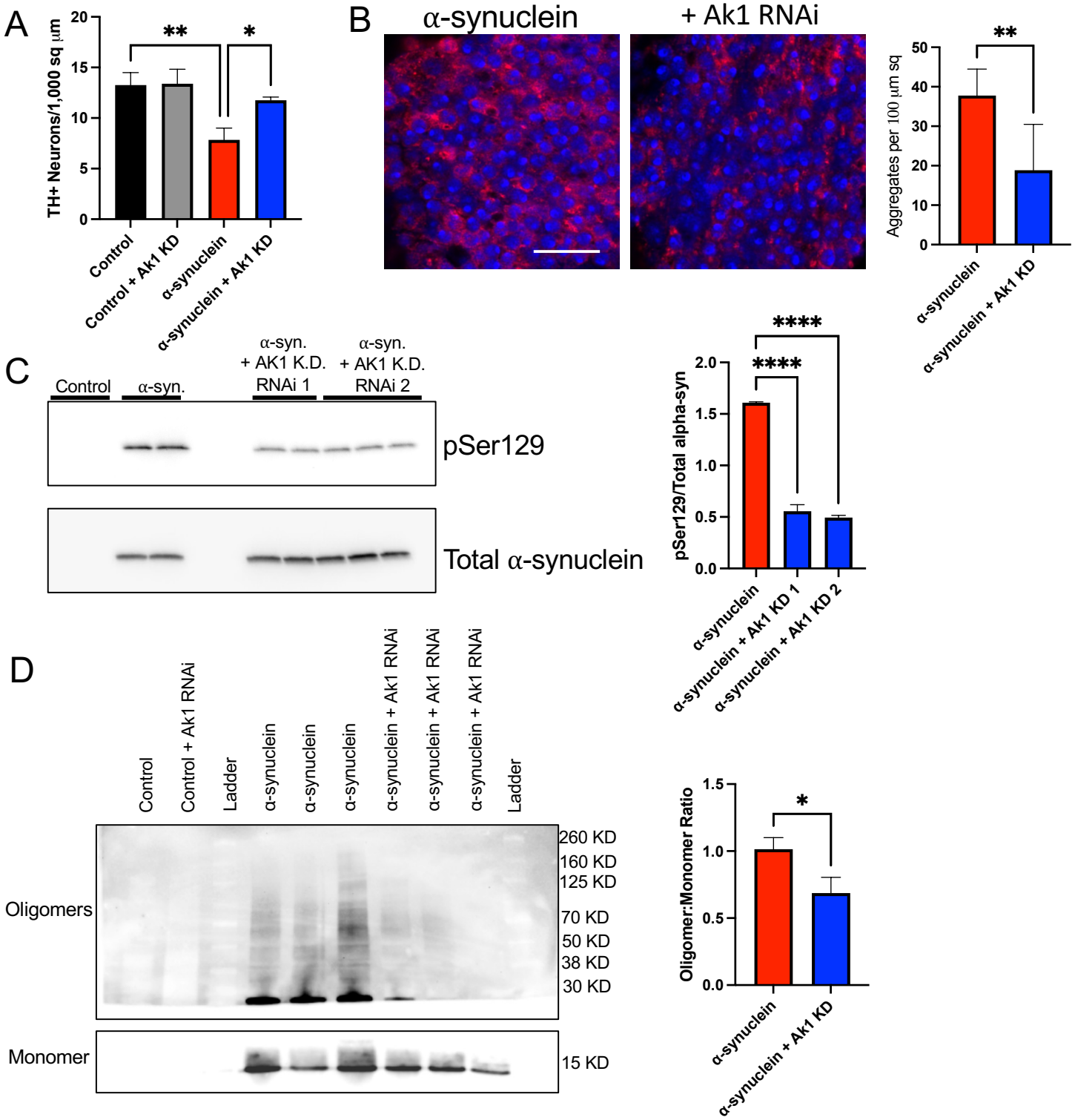

Figure 5

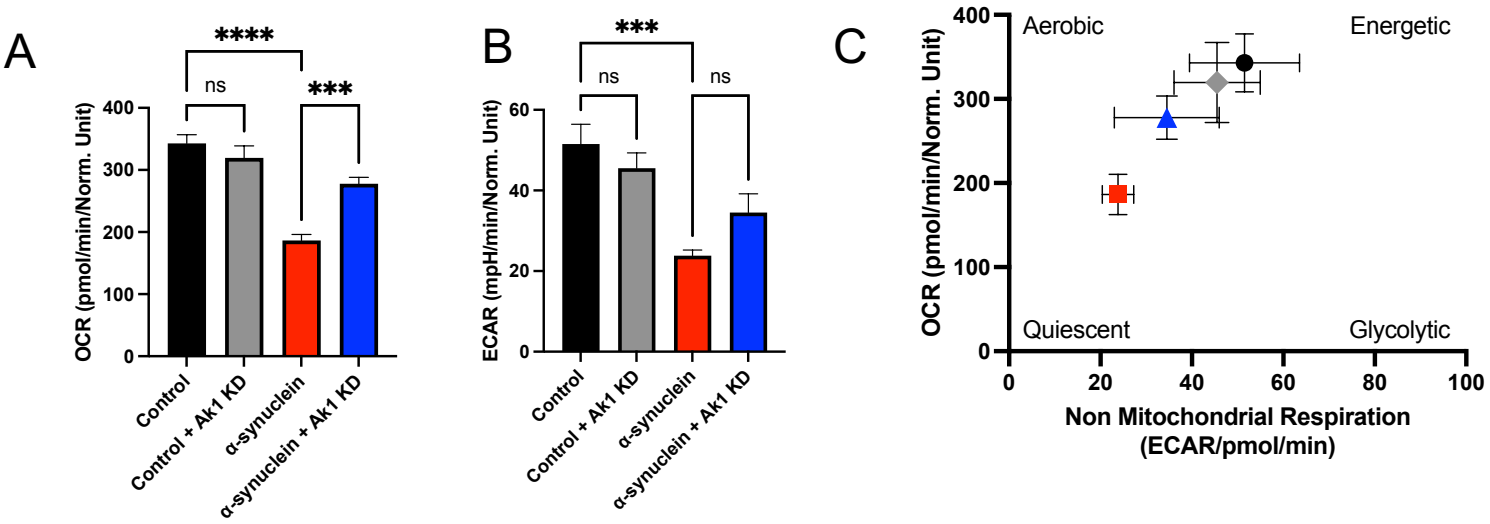

Figure 6

A

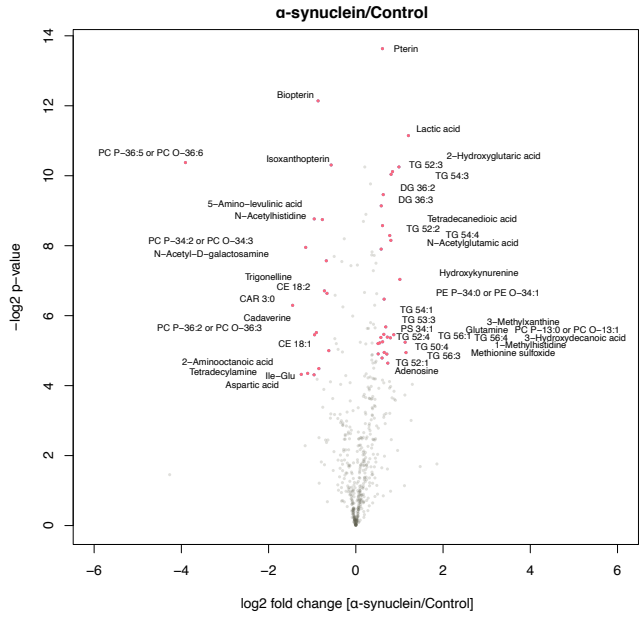

B

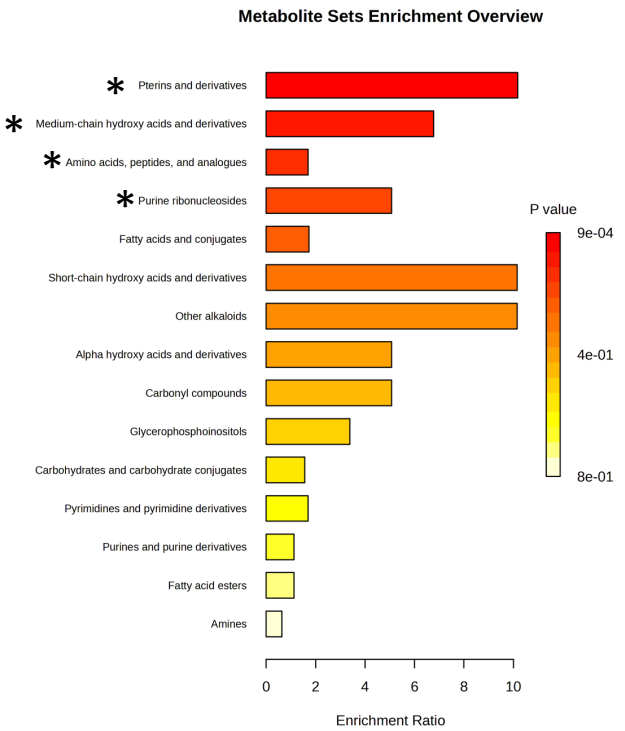

C

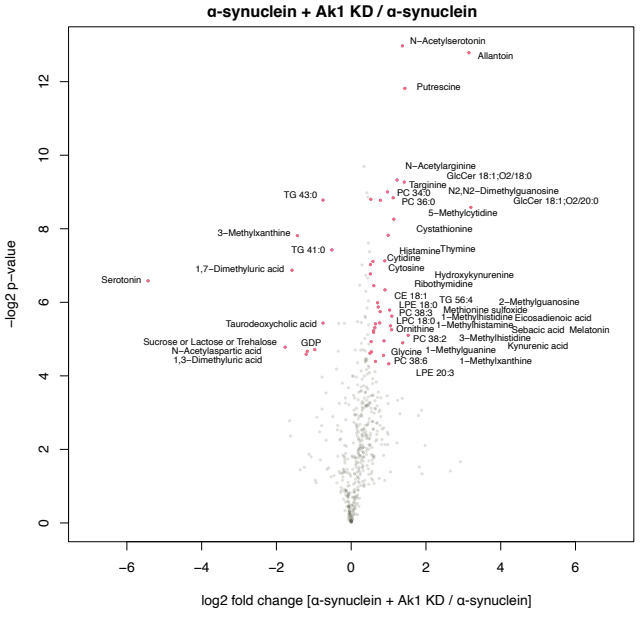

D

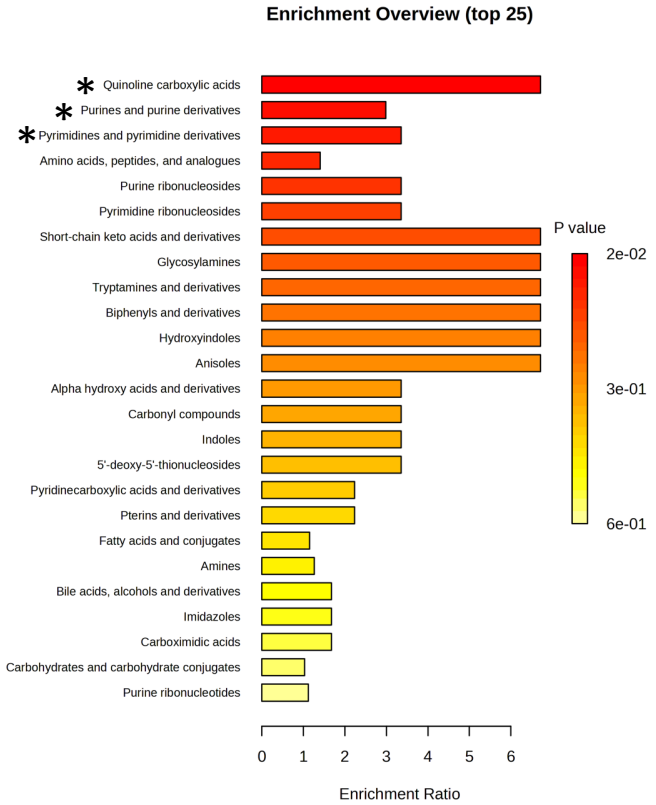

Figure 7

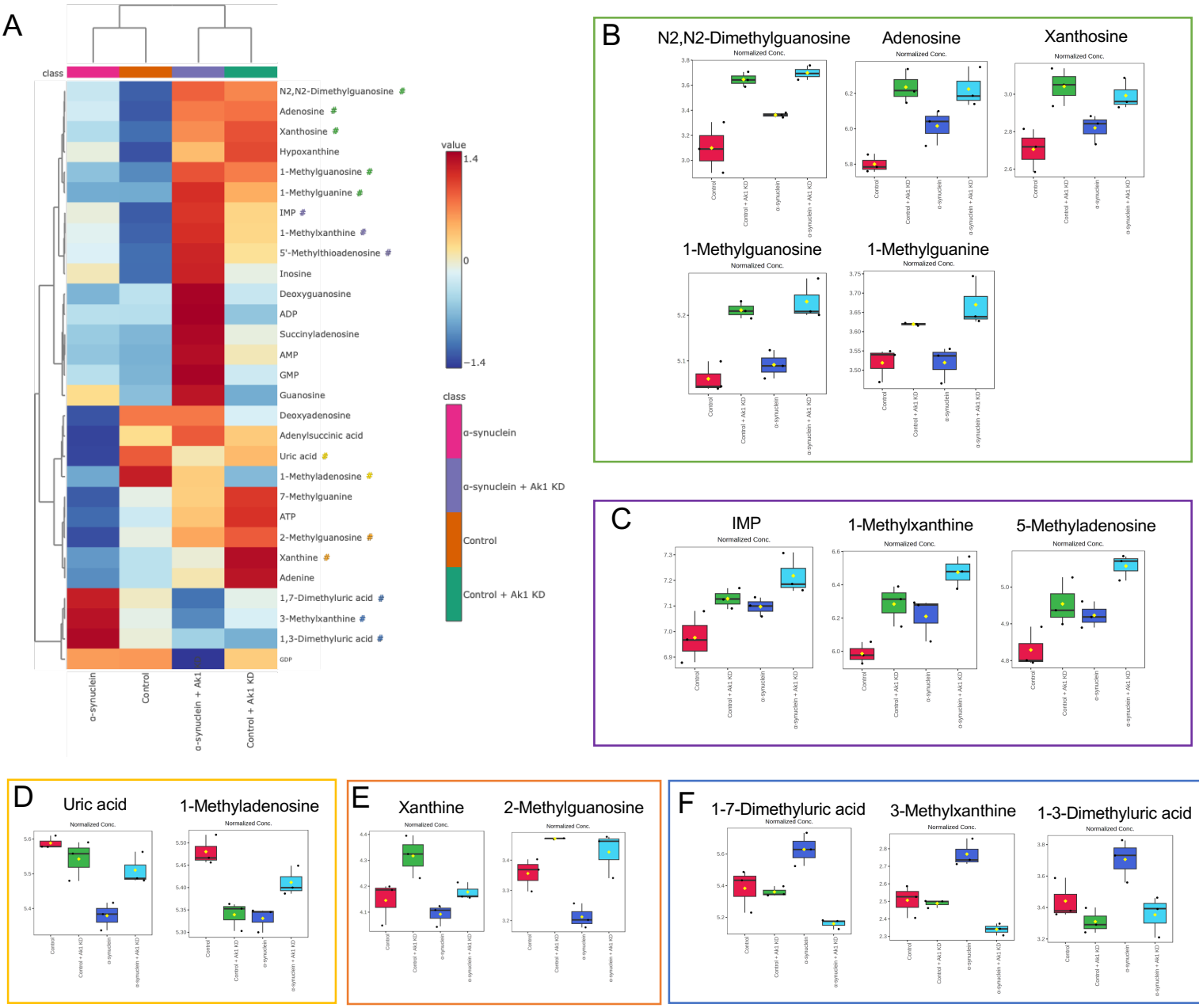

Figure 8

A

Clinical Characteristic	Healthy Controls	Parkinson's disease
Total Number (N)	40	29
Male (N, %)	28, 70%	21, 72.4%
BMI (mean, SD)	25.7, 4.2	26.2, 3.8
Age of onset PD (years, SD)		58.4, 7.9
Disease duration (years, SD)		3.5, 3.1
Total UPDRS (mean, SD)		33, 13.0
Hoehn and Yahr stage (mean, SD)		2.0, 0.3
MMSE (mean, SD)		29.1, 1.2

B